Methanol−Water Mixtures: A Microsolvation Study Using the Effective Fragment Potential Method

Ivana Adamovic[†] and Mark S. Gordon*[,‡]

Department of Physiology, Harvard School of Public Health, Boston, Massachusetts 02115, and Department of Chemistry, Iowa State University, Ames, Iowa 50011

Received: January 28, 2006; In Final Form: June 26, 2006

The formation process of methanol−water mixtures, $(MeOH/H_2O)_n$, $n = 2, 3,..., 8$ is studied at the molecular level using the general effective fragment potential (EFP2) method and second-order perturbation theory (MP2). Extensive Monte Carlo/simulated annealing global optimizations were used to locate global minimum structures for each *n*, for both homo and hetero clusters. Mixing at the microscopic level was investigated, and some general conclusions about the microsolvation behavior of these mixtures are presented. For all of these clusters, incomplete mixing is observed at the molecular level. Low-energy $(MeOH/H_2O)_n$ clusters retain much of their initial structure in the global minima of the mixed clusters.

I. Introduction

In recent decades, there has been increasing theoretical and experimental interest in the properties of alcohol−water mixtures, in particular, the degree to which mixing between the two species occurs at the molecular level. It is well accepted that thermodynamic and kinetic properties, such as entropy increase, compressibility, and mean molar volume, for these mixtures, are smaller than what would be expected for an ideal mixture of pure liquids.[1] Until recently, these effects were attributed to the "super-structuring" of water and the formation of an ice-like structure in the surrounding water because of the hydrophobic effect of alkyl groups.[2] However, a recent neutron diffraction study by Dixit et al.[3] provides strong evidence that the main reason for the unusual behavior of water−methanol mixtures is incomplete mixing at the molecular level and retention of the network structure of bulk water. Their study showed that the addition of water to methanol has the net effect of pressing methyl groups closer together, while pushing hydroxyl groups apart, and also that the local structure of water in a water−methanol mixture is very similar to that in pure water.

Several theoretical and experimental studies have contributed additional evidence for the incomplete mixing of water−alcohol clusters at the molecular level. A combined experimental−theoretical analysis, using X-ray spectroscopy and theoretical prediction of the X-ray emission spectra[4] by Guo et al.[5] suggested incomplete alcohol−water mixing at the microscopic level, even though it is well-known that alcohols are "fully soluble" in water. Comparing theoretical and experimental X-ray spectra, these authors conclude that water molecules are bridging chains or rings comprising 6−8 methanols. Their results confirm that methanol molecules in solution persist in structures similar to those found in the pure liquid. This study found no evidence for "free-swimming" water molecules that are not involved in hydrogen bonding. A molecular dynamics (MD) study by Wensink et al.[6] was done on mixtures of water and several alcohols: methanol, ethanol, and 1-propanol, using the TIP4P[7] potential for water and the OPLS[8] potential for alcohols. Their study focused on the viscosity and diffusion properties of these mixtures; they concluded that although these potentials can reproduce experimental bulk properties of pure liquids they cannot describe mixtures quantitatively. A combined experimental−theoretical study, using neutron diffraction experiments and MD simulations by Dougan et al.,[9] found that mixtures of water and methanol exhibit extended structures in solution, even though the components are fully miscible. For methanol mole fractions in the range of 0.27−0.54, the experimental and MD data find highly heterogeneous mixing across the entire concentration region, thereby confirming the incomplete mixing theory.

The studies discussed above have served as motivation and guidance for the present work. The main focus of this study is the mixing process between clusters of methanol and water at the molecular level, using two levels of theory, second-order perturbation theory (MP2) and the generalized effective fragment potential (EFP2). Computational methods that incorporate the effects of electron correlation are needed to capture the essential features of the mixing process, but such methods are often too computationally demanding to adequately sample the configuration space, even for small clusters. EFP2 incorporates the essence of electron correlation in an efficient manner, without the need for fitted parameters. The combination of EFP2 configuration sampling and MP2 single point energies accomplishes the primary goal of this study: to understand the mixing process with reliable methods that incorporate electron correlation. A secondary goal is to compare the predictions of the two methods. Damrauer[10] has used the EFP method previously to study the acidity reversal of simple aliphatic alcohols.

II. Computational Methods

A detailed description of the EFP2 method is given elsewhere,[11] so only a brief overview of the method is presented here. As discussed in many previous papers, the EFP2 potential consists of several physically important interaction energy terms. Each of these terms describe either EFP−EFP or EFP−quantum mechanical (QM) interactions. The EFP−EFP part, which is

* Corresponding author. E-mail: mark@si.fi.ameslab.gov.
[†] Harvard School of Public Health.
[‡] Iowa State University.

10.1021/jp060607n CCC: $33.50
Published on Web 08/04/2006

of interest for this study, includes electrostatic (Coulomb),[12] charge penetration,[13] induction (polarization), exchange-repulsion[14,15] and dispersion[16] interactions. The Coulomb interaction is represented by a distributed multipolar expansion (though octopoles), modified by the charge penetration term. The induction interaction, represented by distributed localized orbital polarizability tensors, is iterated to self-consistency. The exchange repulsion is represented by an expansion in the intermolecular overlap, in a localized molecular orbital representation. The dispersion term is obtained by integrating over the (imaginary) frequency-dependent dipole polarizabilities, again in a localized orbital framework. This is the first study of the ability of the EFP2 method to correctly describe the heterogeneous mixing of two molecular species, so it is also an important test of the method. In a previous study of the styrene−styrene potential energy surface,[17] the ability of the EFP2 method to correctly describe H-bonding and $\pi-\pi$ interactions was demonstrated.

The electronic structure code GAMESS[19] was used for all of the calculations presented here. EFP2 potentials were generated for water and methanol monomers. All parameters for the EFP2 potentials were generated using the 6-311++G (2d,2p) basis set, and geometries for methanol and water molecules are provided in the Supporting Information. Multipole moments for the distributed multipolar analysis (DMA)[11,12] were extracted from second-order perturbation (MP2)[20] theory calculations of the first-order density matrix. The charge penetration term[13] was omitted in this work because of a failure of the optimization algorithm for clusters with $n > 2$. The development of a more robust optimization algorithm is currently in progress.

To locate global minima for water, methanol, and water−methanol mixtures, Monte Carlo/simulated annealing (MC/SA)[21−23] simulations were performed. In general, the MC/SA simulations sample a great many structures, retaining those that produce energies that are competitive with the energies of structures determined previously. One can (and does) perform geometry optimizations on the most promising structures. To maximize the likelihood that a global minimum, and all low-lying local minima, have been found, MC/SA runs are initiated from several starting structures. In this manner, tens of thousands of structures are sampled. More details concerning these calculations will be given in Section III. To calibrate the EFP2 method, MP2 single point energies, as well as full and constrained geometry optimizations, were performed for several low-energy clusters consisting of two H_2O and two MeOH molecules. For constrained MP2 optimizations, the internal MeOH and H_2O geometries were fixed at the corresponding monomer geometries for compatibility with the EFP2 method, because EFP2 internal structures are kept frozen. EFP2 and MP2 Hessians (energy second derivatives) were performed at all optimized geometries to ensure that stationary points are indeed local minima.

III. Results and Discussion

This section is divided into subsections as follows: Section III.A. presents a comparison of the EFP2 and MP2 methods, using mixing of two water and two methanol molecules as a test system. Section III.B. considers the same mixing process, formation of $n(MeOH/H_2O)$ for $n = 3, 4, ..., 8$, using the EFP2 method for geometry optimizations and MP2 single point energies at the EFP2 optimized structures. A single summary table with the details at hydrogen bonding and relative energies of all isomers are given on the end of this section. Geometries of all presented isomers are given in the Supporting Information.

A. $n = 2$. MC/SA global optimizations were first performed on separate water and methanol dimers to obtain the lowest energy $(H_2O)_2$ and $(MeOH)_2$ isomers. These simulations were performed starting from different initial geometries and simulation conditions. The temperature range was 9000−300 K. The EFP2 monomers were allowed to move in a box size of $10 \times 10 \times 10$ Å^3. Local (Newton−Raphson) optimizations were performed after some number (typically 10−50) of MC/SA steps. Once the lowest energy separated water and methanol dimers were determined, these dimers were placed ∼5 Å apart and global optimization runs (MC/SA) were performed on the combined system. As an extra test that the lowest energy isomer of the mixed water−methanol system was indeed found in these calculations, MC/SA simulations were also carried out starting from several random orientations of premixed clusters: $(MeOH/H_2O)_2$. In the ideal case, the starting geometry should not be important for the location of the lowest energy isomer. Because the conformational sampling algorithm is not perfect, the importance of choosing a wide range of initial structures, to capture all relevant low-lying energy isomers, will be demonstrated and stressed through out this work.

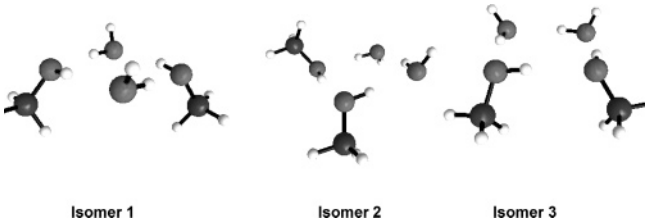

Figure 1. Lowest energy clusters for $n = 2$; EFP2 (MP2//6-311++G (2d,2p)).

TABLE 1: Relative Energies (kcal/mol) for Three $n = 2$ Isomers: MP2, Basis Set: 6-311++G (2d,2p)

isomer	EFP2	MP2/EFP	MP2 optimization
1	0.00	0.00	0.00
2	0.001	−0.02	−0.05
3	0.52	0.71	0.77

The three lowest energy structures for $n = 2$ are shown in Figure 1. These structures are representative snapshots, resulting from extensive MC/SA simulations, starting from different initial structures. Isomer **2** was found in the MC/SA simulations initiated with water and methanol dimers ∼5 Å apart, while isomers **1** and **3** were obtained during MC/SA simulations on the premixed clusters of water and methanol molecules. The energy differences among the three isomers in Figure 1 are very small, less than 1 kcal/mol (Table 1), so all three structures would be relevant in the description of the bulk properties. Because a major goal of this study is to determine, on the molecular level, possibilities of complete versus incomplete mixing, emphasis is placed on the existence and energetics of the lowest energy minima and not on finding all possible isomers for mixed systems. Because the isomers shown in Figure 1 are the lowest energy isomers for the $n = 2$ system, the fact that "incompletely mixed" structures (isomers **2** and **3**) are among them is initial support for the incomplete mixing at the molecular level.

The $(MeOH/H_2O)_2$ system is small enough to easily perform MP2 optimizations on it. Table 1 gives EFP2 and MP2 relative energies for the three lowest energy isomers (Figure 1). All three sets of relative energies are in excellent agreement.

As may be seen in the Supporting Information, although the relative energies and hydrogen-bonding patterns predicted by EFP2 and MP2 are in good agreement for these three isomers, the two sets of geometries are not in as good agreement. For example, EFP2 systematically overestimates the

H-bond distances by ∼0.26 Å, due in part to the omission of the charge penetration term. However, because this overestimation is systematic, and because EFP2 reproduces the essential features of the shapes and hydrogen bonding patterns of the clusters, it is concluded that the method is useful for providing a qualitative and semiquantitative picture of the behavior of these clusters. Hence, for the larger systems only EFP2 optimizations augmented with MP2 single point energies are performed.

The mixing energy for isomer **2** (global minimum at the MP2 level of theory), ΔE_{mixing}, was calculated as the energy difference between the $(MeOH/H_2O)_2$ cluster and the lowest energy separated $(MeOH)_2$ and $(H_2O)_2$ clusters. That is, $\Delta E_{\text{mixing}} = E[(MeOH/H_2O)_2] - E[(MeOH)_2] - E[(H_2O)_2]$. It is found that $\Delta E_{\text{mixing}}(\text{EFP2}) = -11.4$ kcal/mol and $\Delta E_{\text{mixing}}(\text{MP2}) = -15.6$ kcal/mol. Because the agreement between EFP2 and MP2 for the relative energies of the isomers (see Table 1) is much better (within 0.5 kcal/mol), the disagreement of ∼4 kcal/mol is surprising. To investigate the possible origin of this disagreement, first, coupled cluster calculations with single and double excitations with perturbative triples (CCSD(T))[24−26] were performed at the optimized EFP2 structures. ΔE_{mixing}[CCSD(T)] = −15.0 kcal/mol, in very good agreement with MP2. Second, the "counterpoise" method was used to correct for a possible basis set superposition error, BSSE. This could be important because the model potential EFP2 has no such error. The calculated BSSE at the MP2 level of theory is ∼1.5 kcal/mol. This is an upper limit because the counterpoise method often over-corrects for BSSE. So, at most, BSSE accounts for about 1/3 of the difference between EFP2 and MP2. Finally, the EFP ΔE_{mixing} was recalculated including charge penetration effects, yielding −13.4 kcal/mol. So, the combination of BSSE and the inclusion of charge penetration in EFP2 accounts for the difference between the two methods. As noted above, the EFP2 geometries are reliable, and the relative energies of different isomers with the same n agree well with the MP2 results, due to cancellation of the charge penetration effect in clusters of similar size. So, for $n > 2$, the strategy will be to perform EFP2 geometry optimizations, followed by MP2//EFP2 single point energies to calculate ΔE_{mixing}.

To further analyze the water−methanol mixing process, an approximate mixing energy was calculated by examining the hydrogen-bonding pattern, upon the formation of isomer **2**. In this process, two new methanol−water H-bonds are formed. The H-bond strengths for different donor−acceptor combinations were calculated using both EFP2 and MP2. The MeOH−MeOH H-bond energy is 5.3 kcal/mol (MP2) and 4.0 kcal/mol (EFP2). The H_2O-H_2O H-bond energy is 4.8 kcal/mol (MP2) and 3.8 kcal/mol (EFP2). With regard to MeOH−water interactions, when MeOH is the donor the H-bond strength is 4.8 kcal/mol (MP2) and 3.6 kcal/mol (EFP2). When H_2O is the donor, the H-bond strength is 5.3 kcal/mol (MP2) and 4.1 kcal/mol (EFP2). Using these data, an estimated energy of mixing can be approximated as the difference in the number and strength of H-bonds broken and formed: ΔE_{mixing}= (no. of broken homo H-bonds × energy of homo H-bond) − (no. of formed hetero H-bonds × energy of hetero H-bond). This gives an approximate ΔE_{mixing} of −7.7 and −10.1 kcal/mol, for EFP2 and MP2, respectively. So, the change in the number and strength of the hydrogen bonds accounts for about 2/3 of the exothermicity due to mixing.

B. *n* = 3−8. On the basis of the results presented in the previous section, the following strategy for studying systems with $n > 2$ was developed: for each value of n, the global energy minima of $(MeOH)_n$, $(H_2O)_n$, and $(MeOH/H_2O)_n$ clusters were determined, starting from several alternative initially well-mixed structures, in extensive MC/SA simulations. Next, an MC/SA global minimum search was also carried out starting from the lowest energy $(H_2O)_n$ and $(MeOH)_n$ clusters placed ∼5 Å apart. For each n, MP2 single point energies were calculated at the EFP2 optimized structures.

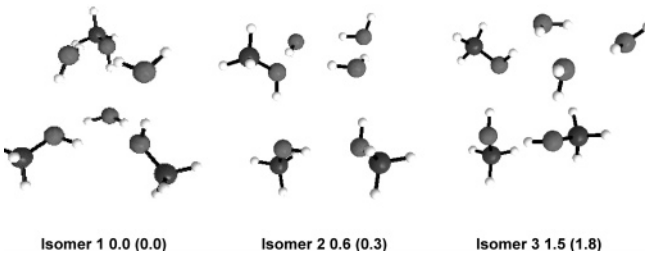

Figure 2. Lowest energy clusters for $n = 3$; **EFP2** (MP2//6-311++G (2d,2p)) (kcal/mol).

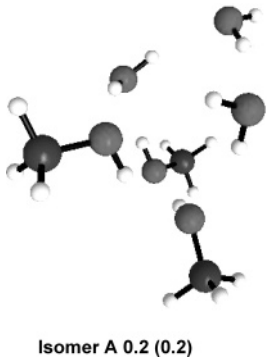

Figure 3. Lowest energy isomer from MC/SA initiated from 3MeOH + $3H_2O$ ∼5 Å apart; **EFP2** (MP2//6-311++G (2d,2p)) (kcal/mol).

The general observation for all n is that at least some of the lowest-energy structures preserve a significant part of the structural characteristics of the separate, unmixed clusters. This observation supports the theory of incomplete mixing at the molecular level, for methanol−water mixtures. The bigger the value of n, the more similarities with the experimental observations were found.

***n* = 3.** Figure 2 illustrates the lowest energy isomers for $n = 3$, with their relative EFP2 (MP2) energies. These structures were obtained from MC/SA simulations, initiated from the well-mixed $(MeOH/H_2O)_3$ clusters. There are many more structures in this energy range, that differ, for example, simply by non-H-bonding hydrogens flipping up and down, but for the sake of space and clarity only these three are presented here.

The MP2 and EFP2 relative energies (Figure 2) are in very good agreement, within less than 1 kcal/mol. Because these four isomers all lie within ∼2 kcal/mol, they could all be important in the mixing processes.

An extensive series of MC/SA global optimizations were also initiated from separate optimized water and methanol clusters, as explained above. This leads to isomers that are structurally different from those shown in Figure 2. The lowest energy isomer found in these MC/SA calculations is presented in Figure 3 (isomer **A**), with the energy given relative to isomer **1**. Note that energies of isomer **1** (Figure 2) and isomer **A** (Figure 3) differ by only ∼0.2 kcal/mol. So, isomer **A** is also relevant when one is considering the mixing process. Extensive sampling of the conformational space is clearly of crucial importance for the proper description of the mixing processes in these systems.

The global minima for separate water and methanol trimers are cyclic structures, with hydrogens (or $-CH_3$ groups) pointing alternatively up and down. Note that in the $(MeOH/H_2O)_2$ system shown in Figure 3, most features of the reactant clusters are conserved: only one homo H-bond has been broken in both

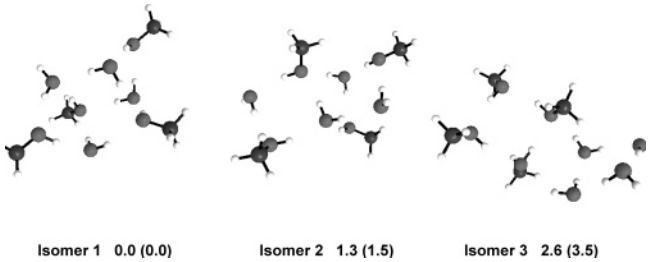

Figure 4. Lowest energy clusters for $n = 4$; **EFP2** (MP2//6-311++G (2d,2p)) (kcal/mol).

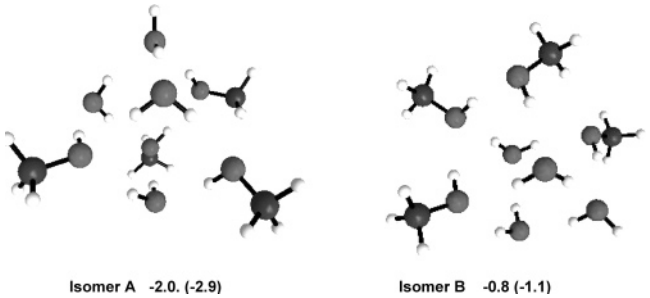

Figure 5. Lowest energy isomer from MC/SA initiated from 4MeOH + 4H_2O ~5 Å apart; **EFP2** (MP2//6-311++G (2d,2p)) (kcal/mol).

water and methanol trimers and two hetero H bonds have formed. This type of behavior has been observed previously[28] for water clusters, and it has been attributed to the strong tendency of H_2O molecules to build H-bonds among themselves, rather than with other molecular species. It is clear, at least for $n = 2,3$, that isomers in which methanol and water clusters retain significant features of their initial structures will play an important role in the mixing processes.

The MP2 energy of mixing for isomer **A**, $n = 3$ is −12.9 kcal/mol. An approximate mixing energy, based on the difference in the number and strengths of H-bonds in the system (as described previously) is −10.4 kcal/mol.

n* = *4. The lowest energy isomers found for $n = 4$ by MC/SA calculations that were initiated from a variety of mixed clusters are shown in Figure 4, together with their relative EFP2 (MP2) energies. Agreement between the two methods is very good, as it is for $n = 2$ and 3.

Figure 5 gives the lowest energy $n = 4$ isomer that was found in the MC/SA calculations starting from separated $(MeOH)_4$ and $(H_2O)_4$ optimized clusters ~5 Å apart (isomer **A**). This isomer is 2.0 (EFP2) or 2.9 (MP2) kcal/mol lower in energy than any of the isomers shown in Figure 4. In addition to isomer **A**, during these MC/SA simulations, an additional structure, which retains the "bulk structure" of isolated $(MeOH)_4$, $(H_2O)_4$ clusters was found. This isomer (isomer **B**, Figure 5) is ~0.8 kcal/mol lower than isomer **1** (EFP2) in Figure 4, and therefore slightly higher in energy than isomer **A**. This illustrates the importance of detailed and systematic sampling of the conformational space as well as the relevance of incompletely mixed structures for the explanation of interesting properties of methanol−water mixtures.

As for $n = 3$, the lowest energy minima for pure methanol and water clusters are cyclic structures, with the non-H-bonding Hs (CH_3s) alternating in up and down positions. In the $(MeOH/H_2O)_4$ global minimum (Figure 5), three water molecules are still interconnected and one water is involved in bridging two MeOH molecules. The arrangement shown in Figure 5 resembles the structure described in the study by Guo et al.;[5] that is, water molecules serve as bridges between smaller MeOH clusters. The MP2 energy of mixing, based on the global minimum (isomer **A**) is −13.0 kcal/mol at the MP2 level of theory, while the approximate MP2 mixing energy, based on the numbers of hydrogen bonds made and broken, is −15.1 kcal/mol.

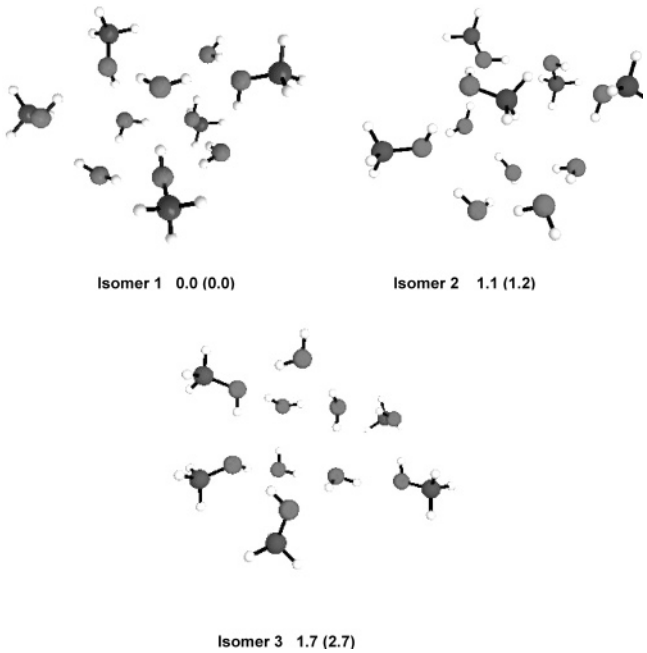

Figure 6. Lowest energy clusters for $n = 5$; **EFP2** (MP2//6-311++G (2d,2p)) (kcal/mol).

Figure 7. Lowest energy isomer from MC/SA initiated from 5MeOH + 5H2O ~5 Å apart; **EFP2** (MP2//6-311++G (2d,2p)) (kcal/mol).

n* = *5. The lowest energy $(MeOH/H_2O)_5$ isomers detected by MC/SA calculations that were initiated from a variety of mixed clusters are shown in Figure 6, together with the corresponding EFP2 (MP2) relative energies. The agreement between the two methods is very good, less than 1 kcal/mol. Note that all of the isomers in Figure 6 have characteristics of unmixed or partially mixed species. For example, one can identify a water tetramer cluster in isomer **1** and a water pentamer cluster in isomer **3**.

The lowest energy $(H_2O)_5$ and $(MeOH)_5$ clusters are still cyclic structures. Figure 7 shows the lowest energy isomer found starting from the separated $(H_2O)_5$ and $(MeOH)_5$ clusters ~5 Å apart (isomer **A**). As for $n = 4$, this isomer is the global minimum on the PES, ~0.5 kcal/mol (EFP2) or 0.2 kcal/mol (MP2) lower than isomer **1** in Figure 6. Isomer **A** retains a considerable amount of the character of the separate $(H_2O)_5$ and $(MeOH)_5$ clusters. Three additional isomers, which retain much of the "pure" cluster structures, and are in the same energy range as the isomers in Figure 6, have been found. Here again, the

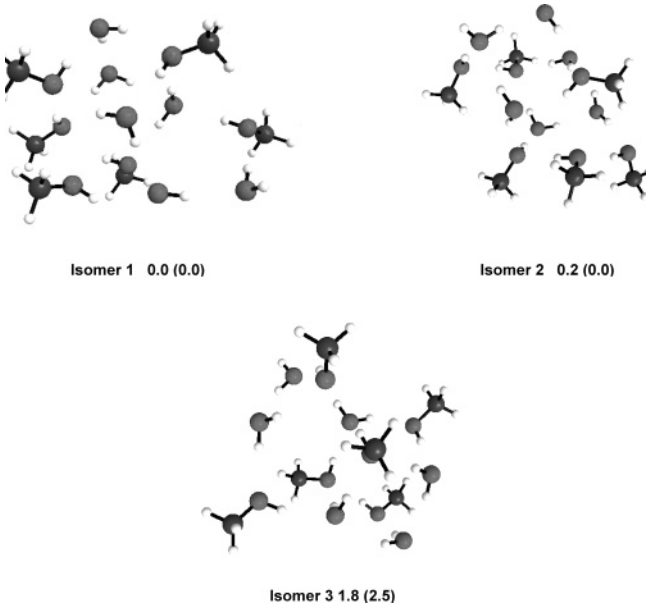

Figure 8. Lowest energy clusters for $n = 6$; **EFP2** (MP2//6-311++G (2d,2p)) (kcal/mol).

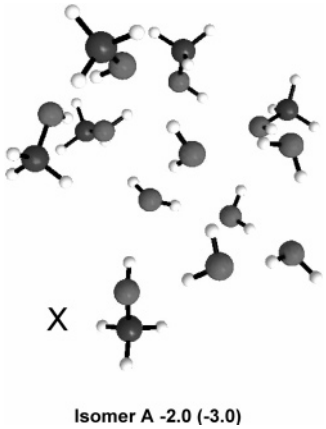

Figure 9. Lowest energy isomer from MC/SA initiated from 6MeOH + $6H_2O$ ∼5 Å apart; **EFP2** (MP2//6-311++G (2d,2p)) (kcal/mol).

existence of many low-energy isomers with retention of structures similar to those of the isolated homo-clusters, support the notion of incomplete mixing. The cluster in Figure 7 has the appearance of a $(H_2O)_5$ cluster that has been inserted into the $(MeOH)_5$ cluster. The mixing energy for this system is −16.0 kcal/mol, while the approximate mixing energy based on the changes in the hydrogen bonds is −20.5 kcal/mol.

***n* = 6.** The lowest $n = 6$ isomers, obtained in the "premixed" MC/SA simulations, are shown in Figure 8. The agreement between the EFP2 and MP2 relative energies is very good, within 1.3 kcal/mol. In all of these structures, $-CH_3$ groups are pointing toward the outer part the cluster, while water molecules are arranged on the inner side, connecting clusters of MeOH together. Even though the MC/SA simulations that led to these species were initiated from mixed structures, it is clear that several waters find each other in the lowest energy structures, leading to incomplete mixing.

The MC/SA global optimization predicts the $(MeOH)_6$ global minimum to be a slightly distorted cyclic structure. The $(H_2O)_6$ global minimum is the "book" structure found previously.[29] The cyclic structure $(H_2O)_6$ is a local minimum on the potential energy surface, ∼2 kcal/mol higher than the global minimum. Starting from the separated $(MeOH)_6$ and $(H_2O)_6$ global minima ∼5 Å apart, extensive MC/SA optimizations were performed. The lowest energy $(MeOH/H_2O)_6$ cluster found in these simulations shown in Figure 9 (isomer **A**) is the global minimum on the PES, lower than isomer **1** (Figure 8) by ∼2.0 (3.0) kcal/mol at the EFP2 (MP2) level of theory. In isomer **A**, water molecules form an H-bond network in which one MeOH molecule (X in Figure 9) is weakly bound to a chain of five other MeOH molecules. All $-CH_3$ groups point away from the polar H_2O cluster that appears to be inserted into the $(MeOH)_6$ complex. The MP2 $n = 6$ mixing energy, based on isomer **A,** is −19.7 kcal/mol, while the approximate mixing energy based

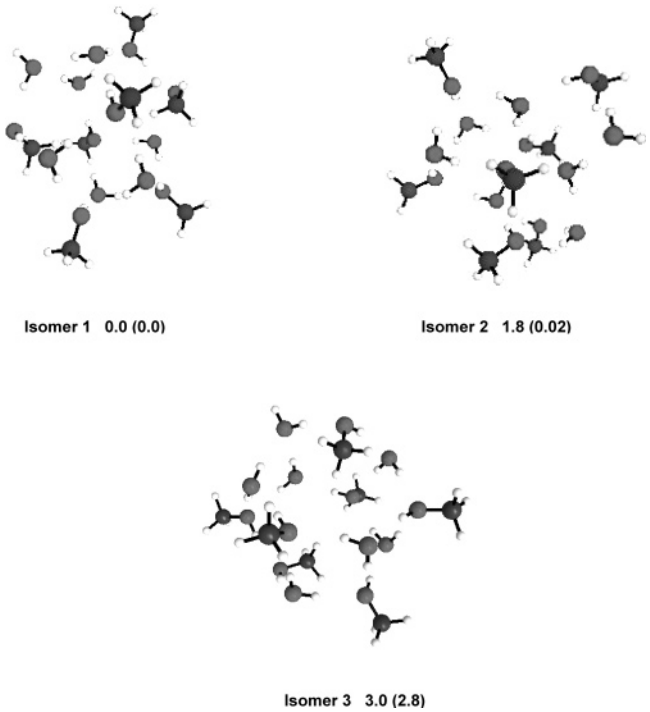

Figure 10. Relative energy for three lowest $n = 7$ isomers; **EFP2** (MP2//6-311++G (2d,2p)) (kcal/mol).

Figure 11. (a) Lowest energy isomers for $(MeOH)_7$ and $(H2O)_7$ clusters; (b) the lowest energy isomer from MC/SA initiated from 7MeOH + $7H_2O$ ∼5 Å apart; **EFP2** (MP2//6-311++G (2d,2p)) (kcal/mol).

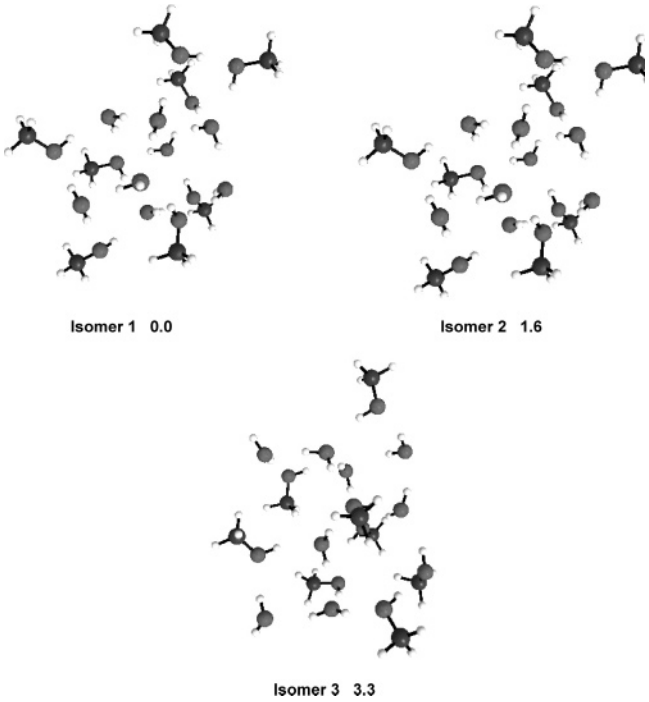

Figure 12. Relative energy for three lowest $n = 8$ isomers; **EFP2** (kcal/mol).

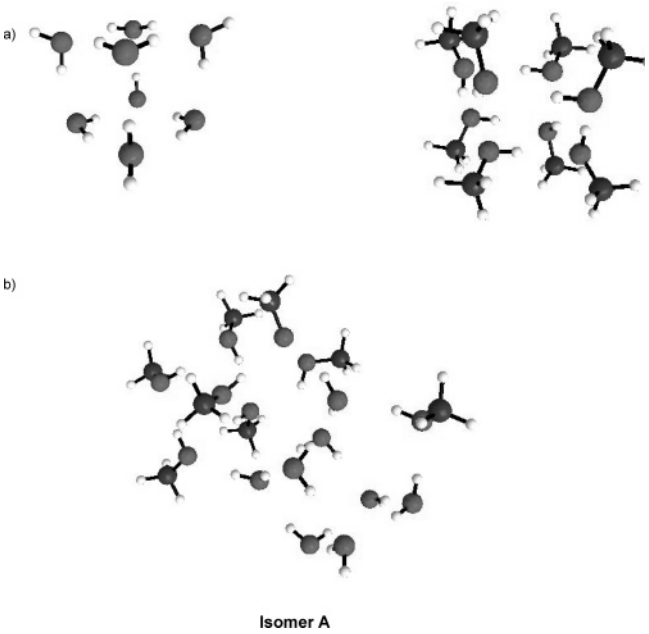

Figure 13. (a) Lowest energy isomers for $(MeOH)_8$ and $(H2O)_8$ clusters (b) Global minimum cluster for $n = 8$.

on the changes in the number of H-bonds of each type is only −10.4 kcal/mol. This disagreement may arise because there are significant changes in the H-bond distances upon formation of the mixed cluster.

***n* = 7.** Figure 10 gives the lowest energy structures for $n = 7$ that were obtained from well-mixed starting structures. Relative energies (Figure 10) at the MP2 and EFP2 level of theory are in very good agreement.

The $(H_2O)_7$ global minimum is a slightly modified book-like structure, whereas the $(MeOH)_7$ global minimum resembles a sphere with $-CH_3$ groups pointing out from the center of the sphere (see Figure 11a). The MC/SA global optimization initiated from these clusters ~5 Å apart results in the structure shown in Figure 11b (isomer **A**). Because the EFP2 (MP2) energy of isomer **A** relative to that of isomer **1** in Figure 10 is only 1.1 (2.6) kcal/mol, it will be relevant for the mixing process. Structure **A** for $n = 7$ has some similarities with structure **A** for $n = 6$ (Figure 9). A water cluster is inserted into the polar, central part of the MeOH cluster, connecting one MeOH molecule with a cluster of six MeOH molecules. This is further evidence for incomplete mixing of water and MeOH clusters and for the existence of water bridges connecting smaller MeOH rings and chains. The MP2 $n = 7$ mixing energy for isomer **A** is −19.2 kcal/mol at the MP2 level of theory, similar to that found for $n = 6$. The approximate mixing energy based on changes in H-bonds is −14.7 kcal/mol.

TABLE 2: Summary of the H-bonding Pattern for $n = 2, 3, ..., 8$; EFP2 Relative Energies (kcal/mol)[a]

	isomer	no. of H_2O-H_2O H-bonds	no. of MeOH−MeOH H-bonds	no. of MeOH (d) − H_2O (a) H-bonds	no. of H_2O(d) − MeOH (a) H-bonds	EFP2 relative energy
	1	0	0	2	2	0.0
$n = 2$	2	1	1	1	1	0.0
	3	1	1	1	1	0.5
	1	1	1	2	3	0.0
$n = 3$	2	2	2	1	2	0.6
	3	3	2	1	1	1.5
	1	1	0	4	6	0.0
$n = 4$	2	1	0	4	5	1.5
	3	4	4	0	2	3.5
	1	1	1	4	8	0.0
$n = 5$	2	5	4	1	2	1.2
	3	5	3	2	4	2.7
	1	4	2	4	7	0.0
$n = 6$	2	5	3	3	6	0.2
	3	4	2	4	7	1.8
	1	2	1	6	11	0.0
$n = 7$	2	2	0	7	11	1.8
	3	1	0	7	11	3.0
	1	5	1	7	10	0.0
$n = 8$	2	4	2	6	11	1.6
	3	6	2	6	8	3.3

[a] (d) H donor; (a) H acceptor.

Because the EFP2 and MP2 relative energies for the low-energy isomers for $n < 8$ are in good agreement, only EFP2 calculations were performed for $n = 8$, with MP2 single point corrections done for the mixing energy.

***n* = 8.** The lowest energy EFP2 isomers for $n = 8$, found by initiating the MC/SA calculations from well-mixed starting structures, are shown in Figure 12. Figure 13a gives the global minima for the separated clusters $(MeOH)_8$ and $(H_2O)_8$. The global energy minimum for $(MeOH)_8$ is a highly symmetric prism-like structure, with four $-CH_3$ groups pointing above and four below the central H-bonded part. The global minimum for $(H_2O)_8$ is also a prism-like structure, as was found previously.[29] The lowest energy $(MeOH/H_2O)_8$ structure found in the MC simulations started from separate methanol and water clusters is isoenergetic with isomer **1** (Figure 13b). Structurally it is very similar to the mixed $n = 6, 7$ clusters labeled **A** in Figures 9 and 11: a water cluster penetrates the hydrophilic central part of the methanol cluster, while the $-CH_3$ groups are pointing away from the center. Water molecules connect opposite ends of the MeOH cluster through their H-bonding network, as observed for $n = 6$ and 7 and also in previous experimental studies.[5] The $n = 8$ MP2 mixing energy is −14.2 kcal/mol, while the approximate mixing energy based on changes in H-bonds is −15.3 kcal/mol.

Summary for n = 2, 3, ..., 8. Table 2 presents a comparison of the relative isomer energies with the topology of hydrogen bonding as a function of *n*. An analysis of this table reveals that the lowest energy isomer for each *n* corresponds to the maximum number of water−methanol intermolecular hydrogen

bonds. Although it is tempting to conclude that this is a general phenomenon, it is important to keep in mind that the energy differences among these isomers are very small.

IV. Conclusions

Mixing processes in water−methanol clusters were studied for the set of $(MeOH/H2O)_n$ mixed clusters, where $n = 2, 3, ..., 8$, using the MC/SA method with the general effective fragment potential (EFP2).

For a given n, EFP2 relative energies of low-lying isomers are in very good agreement with the MP2 method. The MP2 and CCSD(T) $n = 2$ mixing energies are also in very good agreement. Because the EFP2 method reproduces the essential geometrical features of H-bonding patterns in low energy isomers for $n = 2$, EFP2 optimizations followed by MP2 single point energies is a reasonable method for the prediction of the mixing energies in these systems. A new approach to charge penetration that is currently under development is expected to improve the detailed geometrical agreement between the two methods. Estimating the mixing energy using the difference in numbers and strengths of H-bonds in the separate clusters versus the mixed cluster suggests that these changes are the main contribution to the mixing energy.

For all n, a general observation is that there is evidence of incomplete mixing at the molecular level and a tendency of $(H_2O)_n$ and $(MeOH)_n$ clusters to retain their initial structures when the clusters are mixed. This conclusion is based on the existence of low-energy clusters (global minima in most cases) in which MeOH and H_2O molecules tend to retain their identities. Retention of the initial unmixed structure is in good accordance with recent experimental studies[3,5] and supports the incomplete mixing theory at the molecular level.

Acknowledgment. This work was supported by a grant from the Air Force Office of Scientific Research. I.A. acknowledges an NIH training grant, T32HL007118.

Supporting Information Available: Geometries of all presented isomers. This material is available free of charge via the Internet at http://pubs.acs.org.

References and Notes

(1) Murrell, J. N.; Jenkins, A. D. *Properties of Liquids and Solutions*, 2nd ed.; Wiley & Sons: New York, 1994.
(2) Frank, H. S.; Evans, M. W. *J. Chem. Phys.* **1945**, *13*, 507.
(3) Dixit, S.; Crain, J.; Poon, W. C. K.; Finney, J. L.; Soper, A. K. *Nature (London)* **2002**, *416*, 829.
(4) Luo, Y.; Agren, H.; Gel′mukhanov, F. *J. Phys. B: At. Mol. Opt. Phys.* **1994**, *27*, 4169.
(5) Guo, J. H.; Luo, Y.; Augustsson, A.; Kashtanov, S.; Rubensson, J. E.; Shuh, D. K.; Agren, H.; Nordgren, J. *Phys. Rev. Lett.* **2003**, *91*, 157401/1.
(6) Wensink, E. J. W.; Hoffmann, A. C.; van Maaren, P. J.; van der Spoel, D. *J. Chem. Phys.* **2003**, *119*, 7308.
(7) Jorgensen, W. L.; Chandrasekhar, J.; Madura, J. D.; Impey, R. W.; Klein, M. L. *J. Chem. Phys.* **1983**, *79*, 926.
(8) Jorgensen, W. L.; Maxwell, D. S.; Tirado-Rives, J. *J. Am. Chem. Soc.* **1996**, *118*, 11225.
(9) Dougan, L.; Bates, S. P.; Hargreaves, R.; Fox, J. P.; Crain, J.; Finney, J. L.; Reat, V.; Soper, A. K. *J. Chem. Phys.* **2004**, *121*, 6456.
(10) Damrauer, R. *J. Am. Chem. Soc.* **2000**, 122, 6739.
(11) Gordon, M. S.; Freitag, M. A.; Bandyopadhyay, P.; Jensen, J. H.; Kairys, V.; Stevens, W. J. *J. Phys. Chem. A* **2001**, *105*, 293.
(12) (a) Stone, A. J. *Chem. Phys. Lett.* **1981**, *83*, 233. (b) Stone, A. J. *The Theory of Intermolecular Forces*; Oxford University Press: New York, 1996.
(13) Freitag, M. A.; Gordon, M. S.; Jensen, J. H.; Stevens, W. J. *J. Chem. Phys.* **2000**, *112*, 7300.
(14) Jensen, J. H.; Gordon, M. S. *Mol. Phys.* **1996**, *89*, 1313.
(15) Jensen, J. H.; Gordon, M. S. *J. Chem. Phys.* **1998**, *108*, 4772.
(16) Adamovic, I.; Gordon, M. S. *Mol. Phys.* **2005**, *103*, 379.
(17) Adamovic, I.; Li, H.; Lamm, M. H.; Gordon, M. S., in press.
(18) Netzloff, H. M.; Gordon, M. S. *J. Chem. Phys.* **2004**, *121*, 2711.
(19) Schmidt, M. W.; Baldridge, K. K.; Boatz, J. A.; Elbert, S. T.; Gordon, M. S.; Jensen, J. H.; Koseki, S.; Matsunaga, N.; Nguyen, K. A.; et al. *J. Comput. Chem.* **1993**, *14*, 1347.
(20) Moller, C.; Plesset, S. *Phys. Rev.* **1934**, *46*, 618.
(21) Metropolis, N.; Rosenbluth, A. W.; Rosenbluth, M. N.; Teller, A. H.; Teller, E. *J. Chem. Phys.* **1953**, *21*, 1087.
(22) Parks, G. T. *Nucl. Technol.* **1990**, *89*, 233.
(23) Li, Z.; Scheraga, H. A. *Proc. Natl. Acad. Sci. U.S.A.* **1987**, *84*, 6611.
(24) Bartlett, R. J. *Adv. Ser. Phys. Chem.* **1995**, *2*, 1047.
(25) Lee, T. J.; Scuseria, G. E. *Understanding Chem. React.* **1995**, *13*, 47.
(26) Paldus, J. *NATO Adv. Study Inst. Ser., Ser. B* **1992**, *293*, 99.
(27) Boys, S. F.; Bernardi, F. *Mol. Phys.* **1970**, *19*, 553.
(28) Adamovic, I.; Gordon, M. S. *J. Phys. Chem. A* **2005**, *109*, 1629.
(29) Day, P. N.; Pachter, R.; Gordon, M. S.; Merrill, G. N. *J. Chem. Phys.* **2000**, *112*, 2063.